THE JOURNAL OF BIOLOGICAL CHEMISTRY VOL. 287, NO. 24, pp. 20443–20455, June 8, 2012

ARF6 Activated by the LHCG Receptor through the Cytohesin Family of Guanine Nucleotide Exchange Factors Mediates the Receptor Internalization and Signaling*[S]

Received for publication, March 15, 2012, and in revised form, April 5, 2012 Published, JBC Papers in Press, April 20, 2012, DOI 10.1074/jbc.M112.362087

Venkateswarlu Kanamarlapudi[‡1], **Aiysha Thompson**[‡], **Eamonn Kelly**[§], **and Andrés López Bernal**[¶]

From the [‡]*Institute of Life Science, College of Medicine, Swansea University, Singleton Park, Swansea SA2 8PP, United Kingdom, the* [§]*School of Physiology and Pharmacology, University of Bristol, University Walk, Bristol BS8 1TD, United Kingdom, and the* [¶]*Division of Obstetrics and Gynaecology, School of Clinical Sciences, University of Bristol, Henry Wellcome Laboratories for Integrative Neuroscience and Endocrinology, Bristol BS1 3NY, United Kingdom*

Background: The mechanisms by which ARF6 regulate LHCGR internalization and signaling are unknown.
Results: Heterotrimeric G-protein, PI 3-kinase, cytohesin ARF GEFs and ARF GAPs function upstream whereas dynamin and clathrin act downstream of ARF6 in the regulation of HLHCGR internalization and signaling.
Conclusion: Dissected the molecular mechanisms underlying ARF6 involvement in LHCGR internalization and signaling.
Significance: This study provides insight into the mechanisms responsible for HLHCGR regulation by ARF6.

The luteinizing hormone chorionic gonadotropin receptor (LHCGR) is a G_s-coupled GPCR that is essential for the maturation and function of the ovary and testis. LHCGR is internalized following its activation, which regulates the biological responsiveness of the receptor. Previous studies indicated that ADP-ribosylation factor (ARF)6 and its GTP-exchange factor (GEF) cytohesin 2 regulate LHCGR internalization in follicular membranes. However, the mechanisms by which ARF6 and cytohesin 2 regulate LHCGR internalization remain incompletely understood. Here we investigated the role of the ARF6 signaling pathway in the internalization of heterologously expressed human LHCGR (HLHCGR) in intact cells using a combination of pharmacological inhibitors, siRNA and the expression of mutant proteins. We found that human CG (HCG)-induced HLHCGR internalization, cAMP accumulation and ARF6 activation were inhibited by Gallein ($\beta\gamma$ inhibitor), Wortmannin (PI 3-kinase inhibitor), SecinH3 (cytohesin ARF GEF inhibitor), QS11 (an ARF GAP inhibitor), an ARF6 inhibitory peptide and ARF6 siRNA. However, Dynasore (dynamin inhibitor), the dominant negative mutants of NM23-H1 (dynamin activator) and clathrin, and PBP10 (PtdIns 4,5-P2-binding peptide) inhibited agonist-induced HLHCGR and cAMP accumulation but not ARF6 activation. These results indicate that heterotrimeric G-protein, phosphatidylinositol (PI) 3-kinase (PI3K), cytohesin ARF GEF and ARF GAP function upstream of ARF6 whereas dynamin and clathrin act downstream of ARF6 in the regulation of HCG-induced HLHCGR internalization and signaling. In conclusion, we have identified the components and molecular details of the ARF6 signaling pathway required for agonist-induced HLHCGR internalization.

Luteinizing hormone chorionic gonadotropin receptor (LHCGR)[2] is a G-protein-coupled receptor (GPCR) that is mainly expressed in the gonads, where it mediates LH and hCG hormone signaling. Hence LHCGR signaling is important for the maturation and function of the ovary and testis. GPCRs transmit extracellular signals through heterotrimeric G proteins, which consist of $G\alpha$ and $G\beta\gamma$ subunits (1). Agonist-occupation of GPCRs activates the G protein, leading to dissociation of $G\beta\gamma$ from $G\alpha$. $G\beta\gamma$ transmits GPCR signals via downstream effectors such as phosphoinositide 3-kinase (PI3K) (2). PI3K converts PI 4,5-bisphosphate (PIP2) to PI 4,5,3-trisphosphate (PIP3), a second messenger, which recruits to the cell surface and activates proteins containing a pleckstrin homology (PH) domain (3, 4). Wortmannin is a fungal metabolite that acts as a highly selective inhibitor of PI3K (5). The binding of LH or CG to LHCGR results mainly in activation of $G\alpha_s$-coupled adenylyl cyclase. The involvement of G_s-coupled adenylyl cyclase activation and subsequent cAMP accumulation in LHCGR-mediated steroidogenesis is well established (6). It has been shown that LH/CG-induced internalization and subsequent lysosomal degradation of LHCGR is the most important contributor to the down-regulation of this receptor (7).

Most GPCRs are internalized from the cell surface following their activation to dampen the biological response, to recycle and resensitize the receptor through dephosphorylation, or to propagate signals through novel transduction pathways (8).

* This work was supported by BBSRC UK, MRC UK, and the Royal Society UK.
[S] This article contains supplemental Figs. S1–S5.
[1] To whom correspondence should be addressed: Institute of Life Science, College of Medicine, Singleton Park, Swansea SA2 8PP, UK. Fax: 44-1792-602147; E-mail: k.venkateswarlu@swansea.ac.uk.

[2] The abbreviations used are: LHCGR, luteinizing hormone chorionic gonadotropin receptor; LH, luteinizing hormone; CG, chorionic gonadotropin; GPCR, G-protein-coupled receptor; PI, phosphoinositide; PI3K, phosphoinositide 3-kinase; PIP2, PI 4,5-bisphosphate; PIP, PI 3,4,5-trisphosphate; PH, pleckstrin homology; PLC, phospholipase C; GRK, GPCR kinases; ARF, ADP-ribosylation factor; GEF, guanine nucleotide exchange factor; GAP, GTPase-activating protein; BFA, brefeldin A; GGA3, Golgi-associated, γ adaptin ear containing, ARF-binding protein 3; PBD, protein binding domain; EPS15, EGFR pathway substrate clone 15; DN, dominant negative; siRNA, small interfering RNA; DABCO, 1,4-diazabicyclo[2.2.2.]octane; Ro 201724, 4-(3-butuxy-4-methoxybenzyl) imidazolidi2-one; TE, Tris-EDTA; PVDF, polyvinylidene fluoride; EGFR, epidermal growth factor receptor; PBP10, PIP2-binding peptide; PIP5K, PI 4-phosphate 5-kinase.

Agonist-induced GPCR internalization is predominantly mediated by GPCR kinases (GRKs), arrestins, and clathrin-coated pits. GRKs phosphorylate agonist-activated GPCRs to facilitate the recruitment of arrestins, which target GPCR to clathrin-coated pits for rapid internalization (9). Dynamin GTPases plays a key role in agonist-induced GPCR internalization by inducing the fission of clathrin-coated vesicles. However, in the case of LHCGR, formation of the receptor/arrestin complex depends mostly on the agonist-induced activation of the LHCGR rather than on the phosphorylation of the LHCGR (10) and the ARF6 small GTPase plays a critical role in the recruitment of β-arrestin (11). In the follicular membrane, the agonist-stimulation of LHCGR results in ARF6 activation and release of arrestins from the plasma membrane, making it available for binding to LHCGR with subsequent internalization of the receptor (11).

ARF6 is a member of the ARF family of small GTPases, which regulate multiple cellular events by cycling between active GTP- and inactive GDP-bound forms. ARFs depend on guanine nucleotide exchange factors (GEFs) for activation and GTPase activating proteins (GAPs) for inactivation. Among the six known mammalian ARF isoforms (ARFs1–6), ARF1 and ARF6 are the best characterized. ARF1 localizes to and acts at the Golgi whereas ARF6 localizes to and acts at the cell periphery. ARF6 mediates cell surface receptor internalization and reorganization of the actin cytoskeleton beneath the plasma membrane (12). Brefeldin A (BFA), a fungal toxin, inhibits activation of ARFs1–5 but not ARF6 (13, 14). However, ARF6 activation by the cytohesin family of ARF GEFs is inhibited by SecinH3, a cell permeable triazole compound (15). On the other hand QS11 is a cell permeable purine derivative that can increase endogenous ARF1-GTP and ARF6-GTP levels in cells by inhibiting ARF GAP activity (16). There are four cytohesin family members in humans (cytohesins 1–4), each of which contain a PH domain that binds to PIP3. Cytohesins 1–3 translocate from the cytoplasm to the plasma membrane in a PI3K-dependent manner, where they activate ARF6 (6, 17–21).

It is well established that the agonist-induced internalization of LHCGR and several other GPCRs requires ARF6-regulated recruitment and/or activation of several proteins, implicating ARF6 as the central regulator of receptor internalization (11, 22). However, the mechanisms by which ARF6 regulate agonist-induced GPCR internalization remain incompletely understood. Here we investigated the molecular details by which ARF6 regulates agonist-induced HLHCGR internalization using various pharmacological inhibitors and genetic mutants. Our studies demonstrate the activation of ARF6 by agonist-occupied HLHCGR through G$\beta\gamma$, PI3K, and cytohesin ARF GEFs, and the involvement of activated ARF6 in HCG-induced HLHCGR internalization through PIP2, clathrin, NM21-H1, and dynamin. In addition we demonstrate a direct relationship between the expression of cell surface HLHCGR and the extent of cAMP signaling.

MATERIALS AND METHODS

Antibodies and Other Reagents—Antibodies used in the experiments were: mouse monoclonal anti-Myc clone 4A6 (Upstate Biotechnology), mouse monoclonal anti-ARF6 3A-1 (Santa Cruz Biotechnology), rabbit polyclonal anti-ARF1 (a gift from Prof. Sylvain Bourgoin, Laval University, Quebec, Canada), fluorophore-coupled secondary antibodies (Jackson ImmunoResearch Lab), alkaline phosphatase-conjugated secondary antibody (Bio-Rad) and horseradish peroxidise (HRP)-conjugated secondary antibodies (GE Healthcare). Phamacological inhibitors SecinH3 and QS11 were obtained from Merck whereas Wortmannin, Gallein, and Dynasore were from Tocris. Lipopectamine 2000 was from Invitrogen whereas mowiol and PIP2-binding protein (PBP10) were from Merck. Enhanced chemiluminescence (ECL) advanced reagent was obtained from GE Healthcare. All other reagents unless otherwise specified were obtained from Sigma-Aldrich.

Plasmids—The plasmid Myc-HLHCGR, which encodes the full-length receptor with an internal Myc tag, (inserted between aa 72 and 73) at its N-terminal end described previously (10). The plasmid NM23-H1 plasmid was constructed by subcloning NM23-H1 cDNA into pCMV-FLAG vector. NM23-H1 H118C was generated by using QuickChange site-directed mutagenesis kit (Stratagene). GST-GGA3 protein binding domain (PBD) and GFP-cytohesin 2 plasmids described previously (23–25). EPS15 (EGFR pathway substrate clone 15) dominant negative (DN) mutant excised from pEGFP plasmid by EcoRI digestion and subcloned into the EcoRI site of pCMV-FLAG vector (26).

siRNA Oligonucleotides—The specific target nucleotide sequences, 5′-TGACAGAGAGCGTGTGAAC-3′ for human ARF1 siRNA and 5′-GCACCGCATTATCAATGACCG-3′ for human ARF6 siRNA were described previously (27, 28). As a control, an siRNA duplex consisting of a unique sequence that does not have significant homology to any mammalian gene sequences was used. The 21 nucleotide siRNA duplexes were synthesized by Eurogentec.

Cell Culture and Transient Transfection—HEK 293 cells were cultured in DMEM (serum-free medium (SFM)) supplemented with 10% fetal calf serum (FCS), 2 mM glutamine, 100 units/ml penicillin, and 0.1 mg/ml streptomycin at 37 °C in a humidified atmosphere with 5% CO_2. Cells were transfected with indicated plasmids or siRNA or plasmids and siRNA using Lipofectamine 2000™ according to the manufacturers' instructions. Cells were split, 1 day after transfection, into poly-L-lysine (0.1 mg/ml) coated 24-well plates (for ELISA and cAMP assays), 6-cm plates and onto poly-L-lysine (0.1 mg/ml) coated 13 mm coverslips placed in wells of 24-well plate (immunofluorescence) used next day for experimentation.

Receptor Internalization Assay—Internalization of HLHCGR was assessed by ELISA as previously described (24). Briefly, HEK293 cells transiently transfected with Myc-tagged HLHCGR were serum starved for 2 h and then incubated without or with HCG 10 IU/ml for 30 min at 37 °C. Where indicated, cells were incubated with the inhibitors for time mentioned in the figure legends at 37 °C prior to stimulation with HCG. The cells were fixed with 3.7% (w/v) paraformaldehyde in TBS (10 mM Tris-HCl, pH 7.5, 150 mM NaCl)) for 5 min, blocked with 1% BSA for 45 min and incubated with an anti-Myc mouse monoclonal antibody for 1 h and alkaline phosphatase-conjugated anti-mouse IgG for 1 h. Cells were then incubated with *p*-nitrophenylphosphate at 37 °C and read color change at 405 nm using a microplate reader.

Immunofluorescence—Intracellular distribution of cell surface HLHCGR was assessed by immunofluorescence as described (24). Briefly, cells serum starved and treated with inhibitors as mentioned above were incubated with an anti-Myc mouse monoclonal antibody for 1 h at 4 °C, stimulated with HCG 10 IU/ml in presence or absence of the inhibitors at 37 °C for 30 min. The cells were fixed with 3.7% (w/v) paraformaldehyde for 30 min, permeabilized using 0.2% Triton X-100, blocked with 1% BSA and then incubated with fluorescence-tagged anti-mouse IgG for 1 h. The cells were mounted on slides with mounting solution (0.1 M Tris-HCl, pH 8.5, 10% mowiol, and 50% glycerol, containing 2.5% DABCO (1,4-diazabicyclo[2.2.2.]octane), and immunofluorescent staining was visualized using a Leica confocal microscope with a 63× oil immersion lens.

cAMP Assay—The cells were serum starved for 2 h and incubated with 0.25 mM concentration of phosphodiesterase inhibitor Ro 201724 at 37 °C for 15 min. The cells were then stimulated with HCG 10 IU/ml for 30 min 37 °C. Where indicated, cells were incubated with the inhibitors for indicated time at 37 °C prior to stimulation with HCG. cAMP levels were then determined as previously described (24).

ARF6 Activation Assay—ARF6 activation was assessed by using the GST-GGA3 PBD (amino acids 1–316) pulldown assay as described previously (25). The GST-GGA3 PBD fusion protein purified and coupled to glutathione beads as described (18). The transfected cells stimulated without or with HCG 10 IU/ml for 30 min at 37 °C in the presence of or absence of inhibitor were lysed using ice-cold lysis buffer (50 mM Tris-HCl, pH 7.5, 150 mM NaCl, 1% Triton X-100, 0.5% sodium deoxycholate, 0.1% SDS, and 10 mM $MgCl_2$) with 1% protease inhibitors mix. The cell lysates were incubated with glutathione-Sepharose beads coupled to 50 μg of purified GST-GGA3 PBD fusion protein at 4 °C for 2 h. The beads were washed three times with the wash buffer (50 mM Tris-HCl, pH 7.5, 10 mM $MgCl_2$, 150 mM NaCl, and 1% Triton X-100). The lysates that not incubated with the beads were used as an input controls. ARF6- or ARF1-GTP bound to the beads and total ARF1 or ARF6 in the inputs were determined by immunoblotting using an anti-ARF6 or an anti-ARF1 antibody. Immunoblots were scanned and the GTP-bound ARF6 precipitated with GST-GGA3 PBD beads was normalized to total ARF6 levels in the lysates to compare ARF6-GTP levels in different conditions.

Immunoblotting—Proteins were separated by SDS-PAGE, transferred onto PVDF membrane and immunoblotted using primary antibody and the HRP-conjugated secondary antibody as described previously (29).

Data Analysis—Image-J program was used for densitometric analysis. Data were analyzed by using the GraphPAD Prism program. Unless indicated otherwise, results were expressed as the mean ± S.E. of three experiments. The confocal images shown in the figures are representative of three different cell preparations.

RESULTS

Involvement of ARF6 in the HCG-induced Internalization of HCGLHR—We transiently transfected HEK293 cells with HLHCGR containing an N-terminal Myc epitope tag (HEK-HCGLHR cells) and first assessed by ELISA both the concentration- and time-dependence of HCG-induced HLHCGR internalization. When added to the cells for 30 min, HCG induced receptor internalization with an EC_{50} of ~8 IU/ml and a maximum of ~45% receptor internalization being observed at 100–1000 IU/ml of the agonist (supplemental Fig. S1*A*). Addition of 10 IU/ml of HCG to the cells led to time-dependent internalization of HLHCGR (supplemental Fig. S1A) with maximum HLHCGR internalization being observed 30–60 min after agonist addition. Immunofluorescence of HEK-HCGLHR cells confirmed the agonist-dependent internalization of HLHCGR. HCG caused a decrease in cell surface expression of HLHCGR and concomitant increase in intracellular bright punctuate spots, indicating internalization of the receptor (supplemental Fig. S1*B*). We next assessed the concentration and time dependence of agonist-induced cAMP production in HEK-HCGLHR cells. The EC_{50} value for HCG-induced cAMP accumulation was 5.1 IU/ml and a maximum 6-fold over basal increase in cAMP accumulation being observed for HCG at 100–1000 IU/ml for 30 min and 10 IU/ml for 60 min (supplemental Fig. S1*C*). Unless otherwise indicated, a standard agonist treatment of 10 IU/ml of HCG for 30 min was used in further experiments.

To understand the role of ARF6 in HCG-induced internalization of HCGLHR, we first analyzed the effect of down-regulation of ARF6 and ARF1 on agonist-induced HLHCGR, using previously validated ARF6 and ARF1 siRNAs (27, 28). The efficiency of down-regulation of ARF6 and ARF1 protein expression in the cells transfected with ARF6 and ARF1 siRNAs, respectively, is shown in Fig. 1*A*. ARF6 expression was significantly depleted (~80%) in the cells transfected with ARF6 siRNA but not in either ARF1 siRNA or universal negative control siRNA-treated cells. Similarly ARF1 expression was considerably reduced (~90%) in ARF1 siRNA treated but not in ARF6 or negative control siRNA-transfected cells. Depletion of ARF1 or ARF6 had no affect on cell surface expression of HLHCGR in unstimulated cells, as assessed by ELISA (data not shown). However, depletion of ARF6 but not ARF1 significantly inhibited HCG-induced HLHCGR internalization (~10% cell surface receptor loss in ARF6 siRNA-transfected cells compared with ~30% in control or ARF1 siRNA-transfected cells) (Fig. 1*B*). This was further confirmed by immunofluorescence analysis (Fig. 1*C*). Agonist-induced HLHCGR internalization, as evident by punctuate staining in the cytosol, was markedly reduced in cells transfected with ARF6 siRNA but not ARF1 siRNA. Next, we investigated the effect of ARF1 or ARF6 depletion on HCG-induced HLHCGR activation by measuring cAMP accumulation (Fig. 1*D*). Basal cAMP levels (12.7 ± 1.8 pmol of cAMP per mg protein) were not affected by depletion of ARF1 (12.4 ± 2.2 pmol of cAMP per mg protein) or ARF6 siRNA (13.1 ± 1.2 pmol of cAMP per mg protein). However, HCG-stimulated cAMP accumulation was greater (8.3 ± 0.5-fold over basal) in ARF6 siRNA- transfected HEK-HLHCGR cells but not ARF1 siRNA (3.5 ± 0.2-fold over basal) or control siRNA (3.4 ± 0.3-fold over basal) transfected cells. These results confirm the role of ARF6 in agonist-induced HLHCGR internalization and signaling.

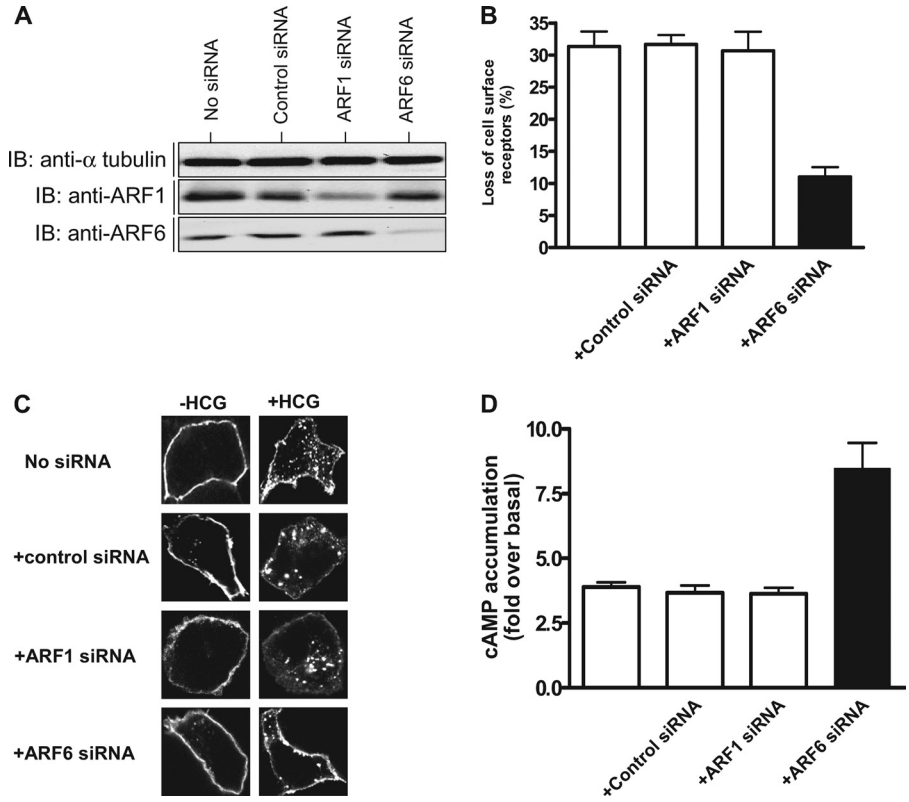

FIGURE 1. **Effect of ARF1 and ARF6 siRNA on HCG-induced HLHCGR internalization and cAMP accumulation.** *A*, immunoblot analysis of the lysates of HEK293 cells co-transfected with HLHCGR (HEK-HLHCGR cells) and 100 nM of control siRNA, ARF1 siRNA, ARF6 siRNA, or nothing, using an anti-ARF1 rabbit polyclonal antibody (pAb), an anti-ARF6 mouse monoclonal antibody (mAb), or an anti-α-tubulin mouse mAb. ARF1 pAb and ARF6 mAb confirm the siRNA-induced down-regulation of ARF1 and ARF6, respectively, while α-tubulin mAb was used as a loading control. *B*, HEK-HLHCGR cells co-transfected with control siRNA, ARF1 siRNA, ARF6 siRNA, or nothing were stimulated with 10 IU/ml HCG for 30 min at 37 °C. The cell surface expression of HLHCGR was determined by ELISA. *C*, immunofluorescence analysis of the effect of ARF1 or ARF6 down-regulation on HCG-induced HLHCGR internalization. HEK-HLHCGR cells co-transfected with or without control siRNA, ARF1 siRNA, or ARF6 siRNA were incubated with an anti-Myc antibody at 4 °C for 1 h following which the cells were incubated in the presence or absence of 10 IU/ml HCG at 37 °C for 30 min. After fixing, the cells were permeabilized, and immunostained using TRITC-conjugated anti-mouse IgG secondary antibody, and the staining visualized by confocal microscopy. *D*, cAMP accumulation in HCG-stimulated (10 IU/ml, 30 min) HEK-HLHCGR cells co-transfected without or with control siRNA, ARF1 siRNA, or ARF6 siRNA.

The *N*-myristoylated ARF1 (Myr-ARF1; composed of 2–17aa of ARF1) and ARF6 (Myr-ARF6; consists of 2–13 aa of ARF6) peptides have previously been shown to inhibit the functions of ARF1 and ARF6, respectively (27, 30). We synthesized the Myr-ARF1 and Myr-ARF6 peptides and made them membrane permeable by coupling them to the cell-permeating domain of the *Drosophila* antennapedia protein (penetratin). The membrane permeable Myr-ARF1 and Myr-ARF6 peptides were used to determine the specificity of ARF6 involvement in HCG-induced HLHCGR internalization in intact cells (31, 32). Treatment of HEK-HLHCGR cells with the Myr-ARF6 peptide but not the Myr-ARF1 peptide or control peptide penetratin inhibited HCG-induced HLHCGR internalization in a concentration-dependent manner with an EC_{50} of 0.5 ± 0.1 μM (Fig. 2*A*). This inhibitory effect of the Myr-ARF6 peptide was confirmed by immunofluorescence (Fig. 2*B*), where Myr-ARF6 but not Myr-ARF1 or control penetratin blocked HCG-induced internalization of HLHCGR. Furthermore, HCG-induced cAMP accumulation was significantly increased from 3.4 ± 0.4-fold to a maximum of ~8.5 ± 1.7-fold, as the concentration of the ARF6 peptide was increased, with an EC_{50} of 0.5 ± 0.2 μM, whereas the ARF1 peptide and penetratin treatment had no effect on HCG-induced cAMP accumulation (Fig. 2*C*).

ARF6 Activation by HCG Stimulation of HEK-HCGLHR Cells—When ARF6 is in its active GTP-bound form, it presumably interacts with downstream effectors in the HLHCGR signaling pathway to promote agonist-induced receptor internalization (11). We used the GST-GGA3 PBD pulldown assay to assess if HCG-stimulation of HEK-HCGLHR cells causes ARF6 activation. The GST-GGA3 PBD specifically binds to the GTP-bound form of ARF and therefore the fusion protein coupled to glutathione beads along with an ARF1- or ARF6-specific antibody has been used to detect activated endogenous ARF1 or ARF6 in cell lysates (23). Upon stimulation with HCG, the levels of endogenous ARF6-GTP, but not ARF1-GTP, are increased in HEK-HLHCGR cells (Fig. 3*A*), indicating that HCG-stimulated HLHCGR selectively activates ARF6 in these cells. We next assessed the concentration- and time-dependent activation of ARF6 in HCG-stimulated HEK-HCGLHR cells (Fig. 3, *B* and *C*). When HCG was added to the HEK-HCGLHR cells for 30 min, ARF6 was activated with increasing concentration of HCG and reached saturation at 100 IU/ml (3.1 ± 0.9-fold over basal). Addition of 10 IU/ml of HCG to the cells led to the time-dependent activation of ARF6 with maximum ARF6 activation (4.1 ± 0.1-fold over basal) being observed 30–60 min after agonist addition. The kinetics of HCG-induced ARF6 activation corre-

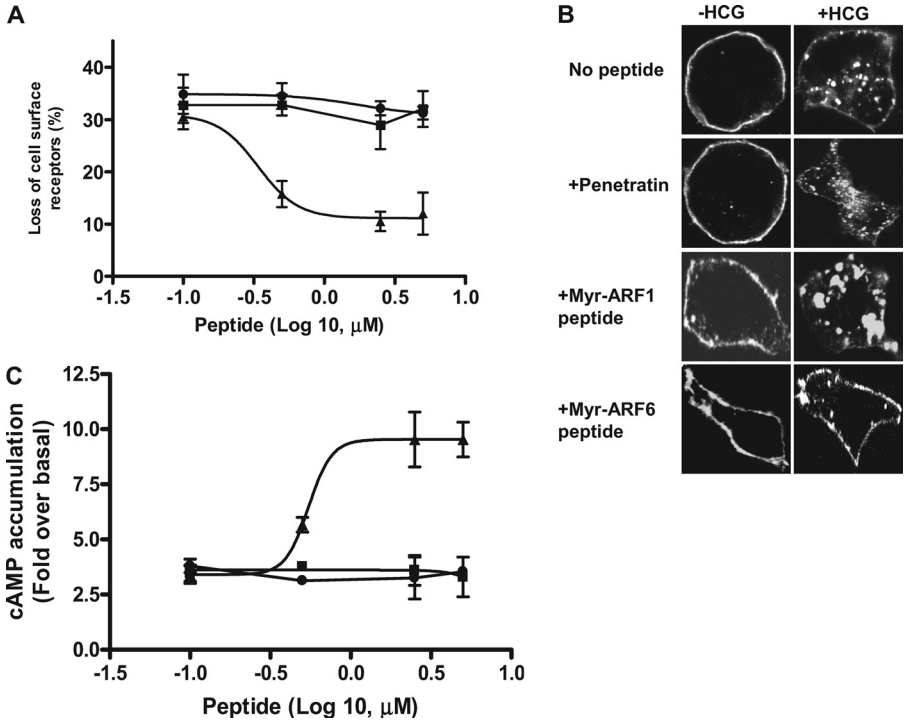

FIGURE 2. **Effect of the MyrARF6 and MyrARF1 inhibitory peptides on HCG-stimulated HLHCGR internalization and cAMP accumulation.** *A*, HEK-HLHCGR cells were incubated with 0.1–5 μM penetratin (■), penetratin-coupled Myr-ARF1 (●) or penetratin-coupled Myr-ARF6 (▲) peptides for 2 h at 37 °C and then incubated in the presence or absence of 10 IU/ml HCG for 30 min. HLHCGR internalization was determined by ELISA. *B*, immunofluorescence analysis showing the HCG-induced (10 IU/ml HCG, 30 min) internalization of HLHCGR cells in the absence or presence of 2.5 μM penetratin or penetratin coupled Myr-ARF1 or Myr-ARF6 peptides. *C*, cAMP accumulation in HCG-stimulated (10 IU/ml HCG, 30 min) HEK-HLHCGR cells in the presence of 0.1–5 μM penetratin, penetratin-coupled Myr-ARF1, or penetratin-coupled Myr-ARF6 peptides.

late with those of HCG-stimulated receptor internalization (supplemental Fig. S1*A*). Furthermore, ARF6 activation in HCG-stimulated HEK-HLHCGR cells was specifically inhibited by the Myr-ARF6 peptide but not the Myr-ARF1 or control penetratin peptide (Fig. 3*D*). These data suggest a critical role for ARF6 activation in the internalization of HLHCGR.

Effect of SecinH3 and QS11 on HCG-stimulated HLHCGR Internalization and cAMP Production—We next used inhibitors of ARF GEFs (SecinH3 and BFA) and an inhibitor of ARF GAP (QS11) to further analyze the effect of ARF6 activation on HCG-induced HLHCGR internalization. SecinH3 prevents the activation of ARF6 by inhibiting the function of the cytohesin family of ARF GEFs whereas ARF6 activation is insensitive to BFA, which instead inhibits the activation of other members of the ARF family (15, 33). QS11 is a broad spectrum ARF GAP inhibitor that prevents ARF6 inactivation (16). Since ARF6 activation is required for HLHCGR internalization, we hypothesized that SecinH3 may decrease and QS11 may increase HCG-induced HLHCGR internalization. Accordingly, HEK-HLHCGR cells were pretreated with or without inhibitor and then analyzed for HCG-induced HLHCGR internalization (by ELISA and immunofluorescence) and cAMP accumulation. SecinH3 inhibited HCG-induced HLHCGR internalization in a concentration-dependent manner, with a maximum decrease of internalization (95.5 ± 0.9%) at a concentration of 60 μM (Fig. 4*A*). BFA did not inhibit HCG-induced HLHCGR internalization even at a concentration (50 μg/ml) that is known to exert a maximal inhibitory effect on ARF1 function (supplemental Fig. S2*A*). Unlike SecinH3, QS11 caused a concentration-dependent increase in HCG-induced receptor internalization, with a maximum increase of the internalization (48.9 ± 0.8%) at a concentration of 12.5 μM (supplemental Fig. S2*A*). These findings were confirmed through visualization of the intracellular distribution of receptor, in response to HCG stimulation (Fig. 4*B* and supplemental Fig. S2*B*). Upon stimulation with HCG, HLHCGR internalization, as determined by the receptor's intracellular redistribution, was markedly reduced in SecinH3-treated cells but increased in QS11-treated cells as compared with that in control DMSO- or BFA-treated cells. SecinH3 increased HCG-induced cAMP accumulation in a concentration-dependent manner with a maximum effect (11.2 ± 0.8-fold over basal) being observed at a concentration of 30 μM HCG (Fig. 4*C*). This demonstrates the prolongation of HCG-stimulated HLHCGR signaling due to inhibition of receptor internalization by SecinH3 treatment. BFA did not affect cAMP accumulation in HCG-stimulated HEK-HLHCGR cells (supplemental Fig. S2*C*). QS11-treated cells had slightly lower levels of cAMP accumulation in HCG-stimulated cells (3.8 ± 0.4-fold over basal) (supplemental Fig. S2*C*).

Effect of Wortmannin (PI3K inhibitor) and Gallein (βγ Inhibitor) on HCG-induced HLHCGR Internalization and cAMP Accumulation—The above experiments have established a role for ARF6 activation in HLHCGR internalization and the time scale of signaling. ARF6 activation involves the recruitment of its GEFs such as cytohesins to the plasma membrane via their binding to PIP_3 (19). PIP_3 is the lipid second messenger produced by PI3K in agonist-stimulated cells (34). PI3K can be activated directly or through GRK2 by $G\beta\gamma$ subunits that dis-

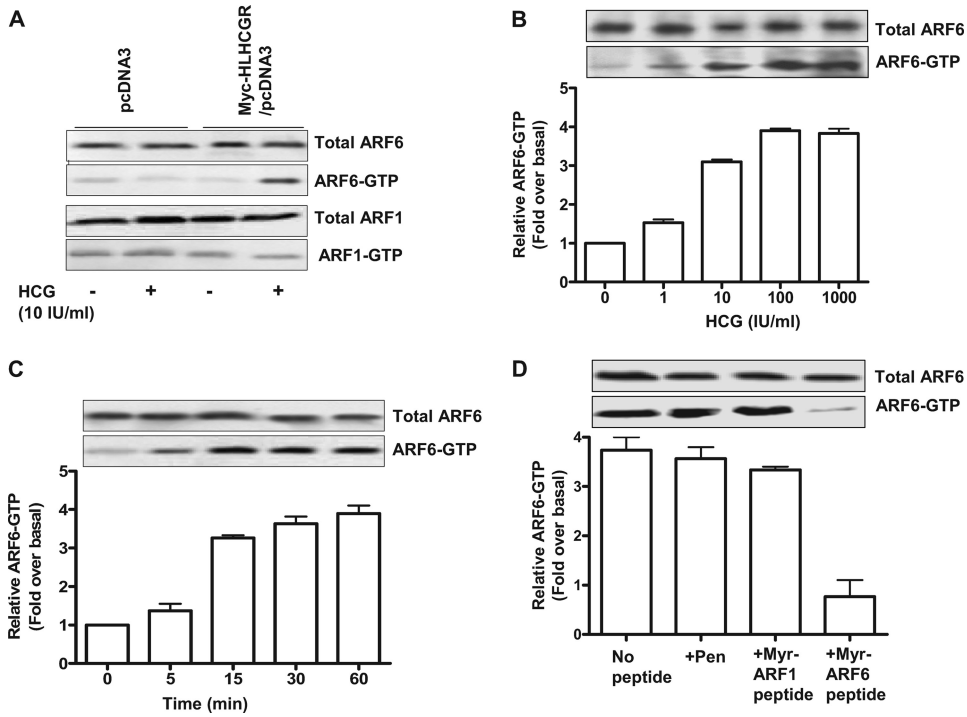

FIGURE 3. **HCG stimulation of HLHCGR induces ARF6 but not ARF1 activation in HEK-HLHCGR cells.** *A*, HEK 293 cells transfected with either pcDNA3 or Myc-HLHCGR were serum starved and treated with or without 10 IU/ml HCG for 30 min at 37 °C. The cells were lysed, and the cell lysates incubated with GST-GGA3 PBD resin to analyze the levels of endogenous ARF1-GTP and ARF6-GTP. Total ARF1 or ARF6 expression in the cell lysates as well as the active ARF1 and ARF6 bound to the resin were detected by immunoblotting using anti-ARF1 rabbit pAb and anti-ARF6 mouse mAb, respectively. *B* and *C*, analysis of concentration- (*B*) and time-dependent (*C*) increase in ARF6 activation in HCG-stimulated HEK-HLHCGR cells. HEK-HLHCGR cells stimulated without or with 1–1000 IU/ml HCG for 30 min or 10 IU/ml HCG for up to 60 min were lysed and subjected to GST-GGA3 PBD pulldown. Total ARF6 and ARF6-GTP were detected by immunoblotting using an anti-ARF6 mouse mAb. Densitometric analysis of the ARF6-GTP is shown as a histogram, after normalizing to the expression of total ARF6 present in the sample. *D*, effect of the Myr-ARF6 inhibitory peptide on ARF6 activation in HCG-stimulated HEK-HLHCGR cells. HEK-HLHCGR cells preincubated for 2 h at 37 °C without (*first lane*) or with 2.5 μM penetratin (*second lane*) or penetratin coupled Myr-ARF1 (*third lane*) or Myr-ARF6 (*fourth lane*) peptides were subsequently stimulated with 10 IU/ml HCG for 30 min, lysed and subjected to GST-GGA3 PBD pulldown to quantify endogenous ARF6-GTP. ARF6-GTP and total ARF6 levels were each assessed by immunoblotting. Densitometric analysis of ARF6-GTP is shown as a histogram, after normalizing to the expression of total ARF6 present in the sample.

sociate from Gα subunit upon agonist binding to the GPCR (35, 36). Wortmannin is a potent inhibitor (IC_{50} <10 nM) of PI3K (37). Gallein efficiently blocks the effects of G$\beta\gamma$ subunits and has a relatively high affinity for interaction with G$\beta\gamma$ (K_d ~400 nM); it disrupts the interactions of G$\beta\gamma$ with downstream binding partners such as PI3K and GRK2 (38, 39).

We therefore studied the effect of Wortmannin and Gallein on HCG-stimulated HLHCGR internalization and cAMP accumulation. Wortmannin concentration-dependently inhibited HCG-induced internalization of HLHCGR from 34.1 ± 1.8% internalization to 13.1 ± 0.9% internalization at 100 nM of the inhibitor (Fig. 4*A*). Gallein treatment also resulted in a concentration-dependent inhibition of agonist-induced receptor internalization from 30.7 ± 1.3% to 15.7 ± 1.3% as the concentration of Gallein increased from 0.4 to 10 μM (Fig. 4*A*). These results demonstrate a direct role for G$\beta\gamma$-activated PI3K in the HCG-induced HLHCGR internalization. These observations were supported by immunofluorescence studies, which demonstrated the inhibition of HCG-induced HLHCGR internalization by Wortmannin and Gallein (Fig. 4*B*). We then investigated the effects of Wortmannin and Gallein on HCG-induced cAMP accumulation. Both Wortmannin and Gallein caused a concentration-dependent increase in HCG-stimulated cAMP accumulation (Fig. 4*C*).

Effect of SecinH3, QS11, Wortmannin, and Gallein on ARF6 Activation by HCG in HEK-HLHCGR Cells—We next analyzed the effect of SecinH3, QS11, Wortmannin and Gallein on ARF6 activation to determine whether these inhibitors might affect HCG-induced HLHCGR internalization via regulation of ARF6. For this purpose, we determined HCG-induced ARF6 activation in HEK-HLHCGR cells pretreated with or without each inhibitor. HCG-stimulated ARF6 activation in HEK-HLHCGR cells pretreated with either BFA or vehicle DMSO was the same as that in untreated cells, as shown by the intensity of the ARF6-GTP bands (Fig. 5*A*). However, SecinH3 inhibited HCG-induced ARF6 activation in HEK-HLHCGR cells in a concentration-dependent manner (Fig. 5*A*). In contrast, QS11 increased ARF6-GTP levels in a concentration-dependent manner in HCG-stimulated HEK-HLHCGR cells (supplemental Fig. S3). The HCG-induced ARF6 activation in HEK-HLHCGR cells was inhibited by Wortmannin and Gallein in a concentration-dependent manner (Fig. 5, *B* and *C*). Together with the results of Fig. 4 and supplemental Figs. S2 and S3, these results indicate that pharmacological inhibition of HCG-induced ARF6 activation reduces agonist-induced HLHCGR internalization.

Effect of SecinH3, Wortmannin, and Gallein on Cytohesin 2 Translocation and HLHCGR Internalization in HCG-stimu-

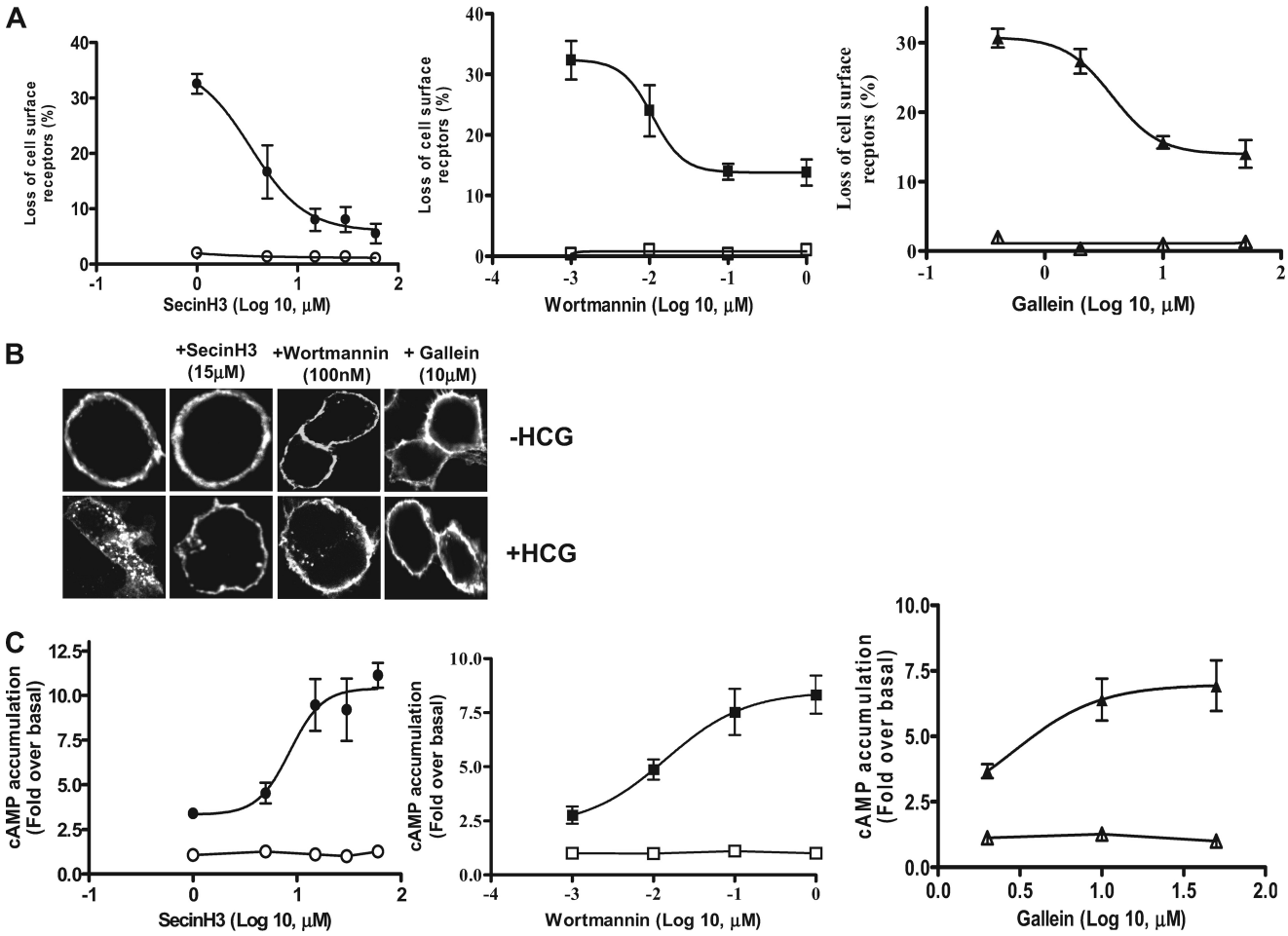

FIGURE 4. **Effect of SecinH3 (ARF GEF inhibitor), Wortmannin (PI3K inhibitor), and Gallein (G$\beta\gamma$ inhibitor) on HCG-induced HLHCGR internalization and cAMP accumulation.** *A*, HEK-HLHCGR cells pre-incubated with either SecinH3 (1–60 μM, ○, ●), Wortmannin (0.001–1 μM, ■, □) or Gallein (0.4–50 μM, Δ, ▲) for 15 min (wortmannin and Gallein) or 2 h (SecinH3) at 37 °C were incubated without (*open symbols*) or with (*solid symbols*) 10 IU/ml HCG for 30 min at 37 °C and receptor internalization determined by ELISA. *B*, immunofluorescence analysis of the effect of SecinH3, Wortmannin and Gallein on HCG-stimulated (10 IU/ml HCG, 30 min) HLHCGR internalization. *C*, cAMP accumulation in unstimulated (*open symbols*) or HCG-stimulated (*solid symbols*; 10 IU/ml HCG, 30 min) HEK-HLHCGR cells pretreated with the indicated concentrations of SecinH3, Wortmannin, or Gallein as described in *part A* above.

lated HEK-HLHCGR Cells—We have previously shown the PI3K-dependent translocation of cytohesins 1–3 from the cytosol to the plasma membrane, where they activate ARF6 (18–21, 40). By activating ARF6 at the plasma membrane, cytohesin 2 can regulate the internalization of LHCGR (11). We have now shown that SecinH3, Wortmannin, and Gallein affect HCG-induced HLHCGR internalization by inhibiting ARF6 activation. Since Wortmannin and Gallein do not inhibit ARF6 activation directly, we hypothesized that these inhibitors affect ARF6 activation by inhibiting cytohesin translocation. To test this hypothesis, we analyzed the effect of Wortmannin or Gallein pretreatment on the cellular distribution of GFP-tagged cytohesin 2 in HCG-stimulated HEK-HLHCGR cells. For this purpose, we co-transfected HEK 293 cells with Myc-HLHCGR and either a GFP or GFP-cytohesin 2 plasmid and subsequently analyzed HCG-induced HLHCGR internalization. HCG-induced HLHCGR internalization was slightly higher (~40%) in the GFP-cytohesin 2 expressing HEK-HLHCGR cells than that in control cells expressing either the receptor alone or the receptor with GFP (each ~31%) (data not shown). We then analyzed the localization of GFP-cytohesin 2 in HEK-HLHCGR cells stimulated with and without HCG. As we observed previously (21), GFP-cytohesin 2 localized to the cytosol in the unstimulated HEK-HLHCGR cells whereas HCG-stimulation induced the translocation of GFP-cytohesin 2 to the plasma membrane and the internalization of the surface HLHCGR to the cytoplasm (Fig. 6). Wortmannin and Gallein inhibited HCG-induced HLHCGR internalization as well as GFP-cytohesin 2 translocation, whereas SecinH3 inhibited HCG-induced HLHCGR internalization but not cytohesin 2 translocation. These results suggests that the inhibition of LHCGR internalization by Wortmannin and Gallein is via the inhibition of cytohesin 2 translocation to the plasma membrane, and that due to SecinH3 through a reduction in cytohesin 2-mediated ARF6 activation.

Effect of NM23-H1 and EPS15 DN Mutants, Dynasore, and PBP10 on HLHCGR Internalization and cAMP Accumulation in HCG-stimulated HEK-HLHCGR Cells—It has been shown previously that LHCGR internalization occurs via a clathrin- and dynamin-dependent process (6, 41). The clathrin complex mediates LHCGR internalization whereas dynamin GTPase causes the fission of clathrin-coated vesicles (10). ARF6 promotes clathrin-mediated internalization by recruiting NM23-H1 and/or the adaptor protein AP2 in polarized cells such as

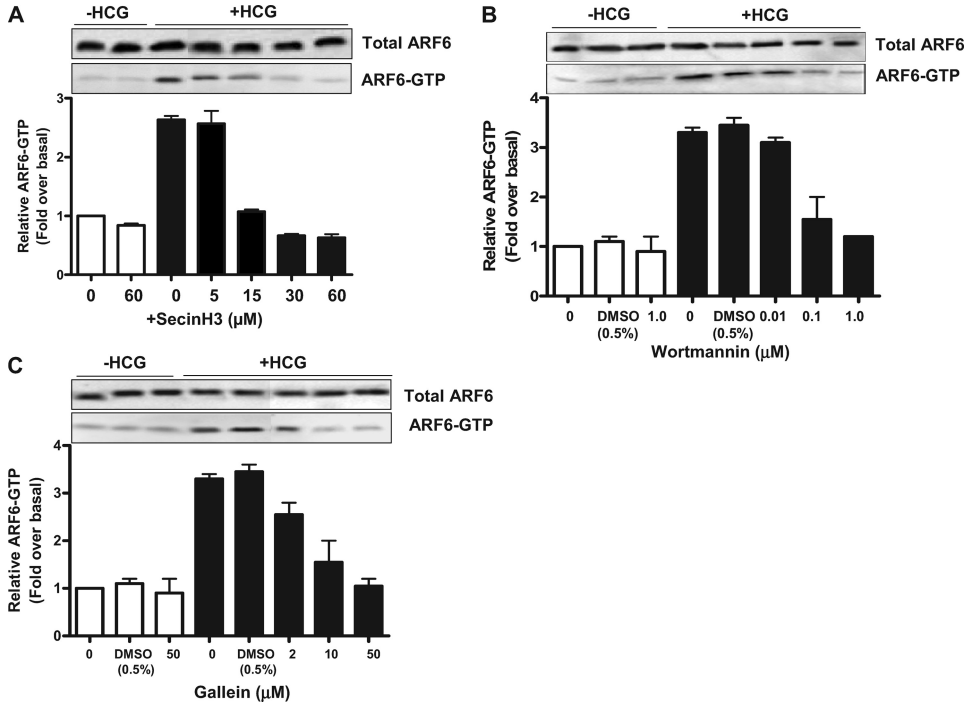

FIGURE 5. **Effect of SecinH3, Wortmannin and Gallein on ARF6 activation in HCG-stimulated HEK-HLHCGR cells.** HCG-stimulated (10 IU/ml HCG, 30 min) ARF6 activation was assessed by a GST-GGA3 PBD pulldown assay in HEK-HLHCGR cells preincubated with the indicated concentrations of (*A*) SecinH3, (*B*) Wortmannin, or (*C*) Gallein. Total ARF6 levels in the cell lysate and the resin bound ARF6-GTP were visualized by immunoblot analysis with an anti-ARF6 mouse mAb. Densitometric analysis of ARF6-GTP is shown as a histogram after normalizing to the expression of total ARF6 present in the sample. For Wortmannin and Gallein, the effect of the drug vehicle (0.5% DMSO) on ARF6-GTP levels, was also determined. *Solid bars* indicate measurements made in the presence of HCG.

neurons and epithelial cells (42). NM23-H1 is a nucleoside diphosphate kinase which activates dynamin-dependent fission of clathrin coated endocytotic vesicles (43). ARF6-GTP binds to and activates PI 4-phosphate 5-kinase (PIP5K)γ, leading to a large increase in PIP2 at the cell surface (44). ARF6-GTP and PIP2 function synergistically to recruit AP-2, suggesting a role for ARF6 in clathrin-coated pit assembly (44, 45). Although ARF6 activation has been linked to the dissociation of arrestin to facilitate LHCGR internalization, a possible direct involvement of ARF6 in clathrin-mediated LHCGR internalization has not been evaluated (11). We hypothesized that ARF6 may regulate HLHCGR internalization by recruiting NM23-H1 to the clathrin-coated pits leading to PIP5Kγ activation. To determine the involvement of this pathway, we assessed the effect of the DN mutants of NM23-H1 (NM23-H1^{H118C}, kinase defective) and EPS15 (EPS15Δ95–295) on HCG-induced HLHCGR internalization (by ELISA and immunofluorescence) and cAMP accumulation, cytohesin 2 translocation and ARF6 activation (26, 43). EPS15, one of the components of the clathrin complex and AP2 interactor, is required for clathrin-dependent endocytosis. Using the same approaches, we also assessed the effect of a cell permeable PBP10 (a decapeptide derived from the PIP2-binding region in segment-2 of gelsolin) and a chemical inhibitor of dynamin (Dynasore) on HCG-induced HLHCGR internalization (46, 47).

Dynasore and PBP10 inhibited HCG-induced HLHCGR internalization in a concentration-dependent manner (supplemental Figs. S4*A* and S5*A*). The cells treated with Dynasore showed a decrease in HCG-induced internalization from 34.0 ± 1.8% to 9.7 ± 1.2% at 80 μM Dynasore (supplemental Fig. S4*A*). PBP10 treatment also resulted in the inhibition of receptor internalization from 28.2 ± 4.0% down to 4.8 ± 2.2% at 10 μM PBP10 (supplemental Fig. S5*A*). These observations were supported by immunofluorescence studies, in which inhibition of HCG-induced HLHCGR internalization by Dynasore and PBP10 was evident (supplemental Figs. S4*B* and S5*B*). Consistent with the internalization results, both Dynasore and PBP10 caused a concentration-dependent increase in levels of HCG-stimulated cAMP accumulation in HEK-HLHCGR cells (supplemental Figs. S4*C* and S5*C*). A significant decrease in HLHCGR internalization and a concomitant increase in HLHCGR-mediated cAMP accumulation was observed in HCG-stimulated HEK-HLHCGR cells co-transfected with either NM23-H1 or EPS15 DN mutants, but not NM23-H1 WT (Figs. 7, *A–C* and 8, *A–C*). Approximately 12% of the cell surface receptor expression was lost in NM23-H1 or EPS15 DN mutant plasmid-expressing cells compared with >30% in control empty plasmid or NM23-H1 WT construct-expressing cells (Figs. 7*A* and 8*A*). This was further confirmed by immunofluorescence analysis (Figs. 7*B* and 8*B*). The agonist-induced HLHCGR internalization, as evident by punctuate staining in the cytosol, was markedly reduced in cells expressing NM23-H1 or EPS15 DN mutant plasmids but not control empty vector or NM23-H1 WT plasmid. Next, we investigated the effects of NM23-H1 and EPS15 mutants on HCG-induced HLHCGR activation by measuring cAMP accumulation (Figs. 7*C* and 8*C*). HCG-stimulated cAMP accumulation was increased in cells expressing NM23-H1 or EPS15 DN mutants but not NM23-H1 WT or control plasmid expressing HEK-HLHCGR cells. HCG-induced cAMP levels in the cells exogenously expressing

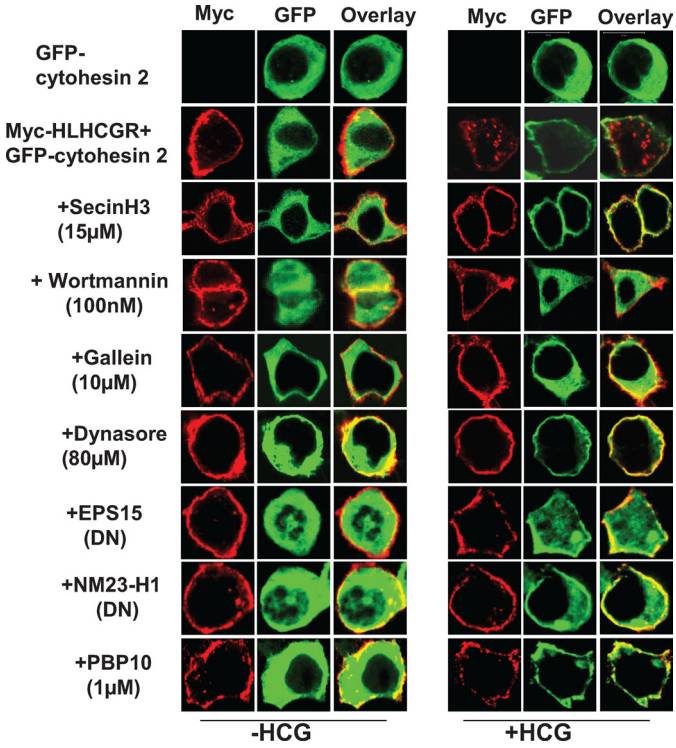

FIGURE 6. **Effect of various inhibitors on cytohesin 2 translocation and HLHCGR internalization in HCG-stimulated HEK-HLHCGR cells.** Immunofluorescence analysis of GFP-cytohesin 2 translocation and receptor internalization in HCG-stimulated (10 IU/ml HCG, 30 min) HEK-HLHCGR cells pretreated for 15 min (Wortmannin, Gallein, and Dynasore) or 2 h (SecinH3) at 37 °C without or with the indicated inhibitor or co-transfected with EP15(DN) or NM23-H1 (*DN*) plasmid. *Red* indicates anti-Myc antibody staining of Myc-HLHCGR, *green* indicates GFP, and *yellow* indicates overlay of *red* and *green*. Note that HCG-induced receptor internalization was inhibited by all drug treatments and co-transfection with the indicated DN plasmid, whereas HCG-induced GFP-cytohesin 2 translocation was inhibited by Gallein and Wortmannin, but not by SecinH3, Dynasore, EPS15 DN, NM23-H1 DN, and PBP10.

NM23-H1 WT were similar to that of the cells transfected with control plasmid. However, the agonist-induced cAMP accumulation was significantly greater in NM23-H1 or EPS15 DN mutant expressing cells. Dynasore, PBP10, NM23-H1 DN, and EPS15 DN had no effect on HCG-stimulated ARF6 activation (Figs. 7*D* and 8*D* and supplemental Figs. S4*D* and S5*D*) or cytohesin 2 translocation in the HEK-HLHCGR cells (Fig. 6). These results indicate that dynamin, PIP2, NM23-H1, and clathrin regulate HLHCGR internalization by acting downstream of ARF6.

DISCUSSION

An important aspect of LHCGR activity and its regulation is the internalization of agonist-activated receptors into the intracellular compartments of the cell (48). ARF6 regulates the internalization of LHCGR as well as that of other GPCRs (11, 22), however, the molecular mechanisms underlying ARF6 involvement in GPCR trafficking are not well understood. In this study we systematically dissected the molecular and cellular mechanisms underlying ARF6 involvement in LHCGR internalization (see summary in Fig. 9). In addition we suggest that the molecular pathways identified here are likely to be shared by other GPCRs where internalization is ARF6-dependent.

The down-regulation of ARF6 expression by siRNA or inhibition of ARF6 by the Myr-ARF6 inhibitory peptide inhibited the agonist-induced internalization of HLHCGR and produced a corresponding increase in agonist-induced cAMP accumulation in HCG-stimulated cells. Similarly, other studies have shown that ARF6 down-regulation inhibits agonist-induced internalization of GPCRs including the β2-adrenoreceptor (β2-AR), M2 muscarinic acetylcholine receptor and the angiotensin II type 1 (AT1) receptor (49), (50, 51). The inhibition of receptor internalization following ARF6 down-regulation causes the receptors to be retained for an increased period on the cell surface, and thus prolongs adenylyl cyclase activation with consequent increases in cellular cAMP accumulation. These results confirm that ARF6 has a crucial role in agonist-induced internalization of HLHCGR, which in turn determines the dynamics of cellular signaling for this receptor.

ARF6 functions by cycling between the inactive GDP- and active GTP-bound conformations, a process which is regulated by GEF and GAP. The active form of ARF6, ARF6-GTP, interacts with downstream effectors in the LHCGR signaling pathway to promote receptor internalization. In this study ARF6 activation by HCG-stimulated HLHCGR was determined using a GST-GGA3 PBD pulldown assay (23, 25, 52). HCG-stimulation of HLHCGR increased cellular levels of ARF6-GTP but not ARF1-GTP, while the Myr-ARF6 peptide but not Myr-ARF1 peptide inhibited HCG-stimulated ARF6 activation. Together these results indicate that HLHCGR specifically activates ARF6, and further implicate ARF6-GTP as a central player in HCG-induced HLHCGR trafficking. Furthermore ARF6 is activated upon agonist-stimulation of other GPCRs including the β2-AR, as well as the follicle-stimulating hormone, M3 muscarinic acetylcholine, fMet-Leu-Phe, H2 histamine, B2 bradykinin, and AT1 receptors (11, 49), suggesting that ARF6-GTP is a central player in the trafficking of many GPCRs.

The cytohesin family of proteins act as GEFs for both ARF1 and ARF6 (53, 17). Although cytohesin 2 is thought to be involved in porcine LHCGR desensitization (11), it is not known whether cytohesin 2 is the ARF GEF responsible for ARF6 activation downstream of LHCGR. In the present study SecinH3, an inhibitor of ARF6 activation by cytohesins, markedly inhibited the agonist-induced internalization of HLHCGR while BFA, an inhibitor of ARFs 1–5 activation, had no such effect. These data indicate that the activation of ARF6 by the cytohesin family of ARF GEFs is a crucial step in HCG-stimulated HLHCGR internalization. Cytohesin 2 is present in follicular membranes at a relatively high concentration and therefore it is possible that cytohesin 2 mediates ARF6 activation downstream of LHCGR in that tissue (54). The ARF GAP inhibitor, QS11, increased HCG-induced receptor internalization presumably by increasing levels of ARF6-GTP. In the cAMP assay, SecinH3 treatment increased while QS11 decreased HCG-stimulated cAMP production, indicating that the length of time that the HLHCGR resides on the cell surface directly determines the ability of this receptor to mediate signaling via G protein. Furthermore, HCG-induced ARF6 activation in HEK-HLHCGR cells was reduced by SecinH3 and moderately increased by QS11. We have previously demonstrated the involvement of the ARF6 GAP centaurin-α1 in β2-adrenoreceptor internalization (24). Centaurin-α1 is likely to play a vital role in GPCR trafficking by modulating the activity of ARF6 (23,

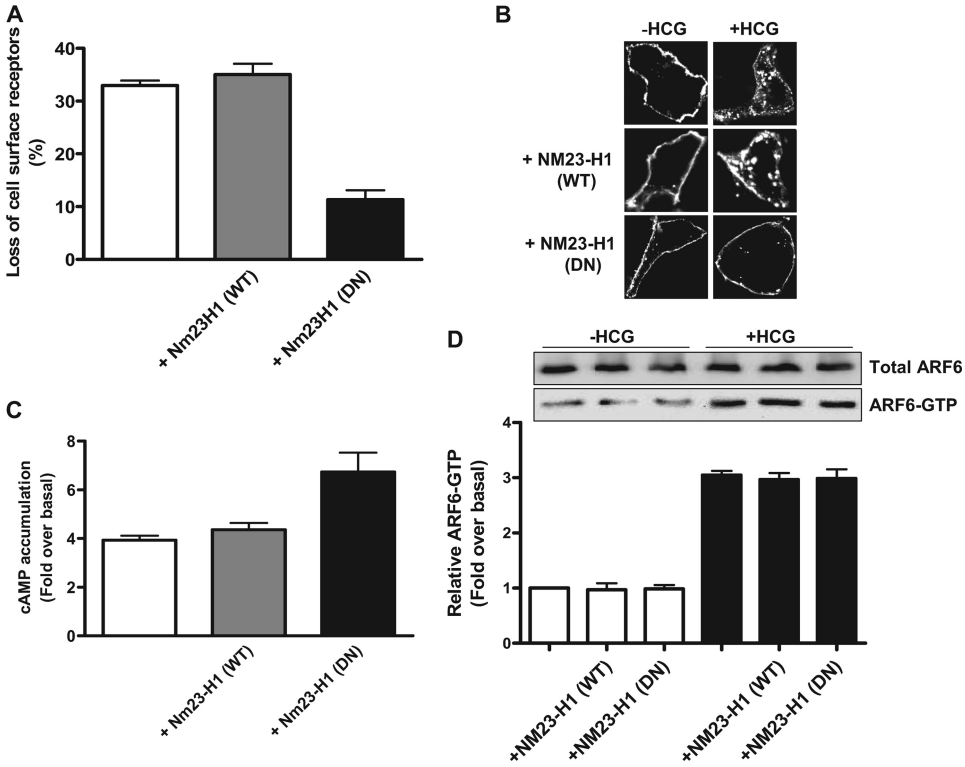

FIGURE 7. **Effect of NM23-H1 DN mutant on HLHCGR internalization and cAMP production in HCG-stimulated HEK-HLHCGR cells.** *A*, HEK-HLHCGR cells coexpressing WT or DN mutant NM23-H1were assayed by ELISA for surface HLHCGR receptor both in the absence and the presence of HCG (10 IU/ml, 30 min). In HCG-treated cells, NM23-H1 DN mutant inhibited HCG-induced receptor internalization. *B*, immunofluorescence analysis showing the inhibition of HCG-stimulated (10 IU/ml HCG, 30 min) HLHCGR redistribution by coexpression of NM23-H1 DN mutant. *C*, cAMP production was increased in HCG-stimulated HEK-HLHCGR cells expressing NM23-H1 DN mutant as compared with cells expressing either NM23-H1 WT or control empty vector. *D*, using a GST-GGA3 PBD pulldown assay, the levels of endogenous ARF6-GTP under basal conditions and in the presence of HCG (10 IU/ml, 30 min) were not affected by coexpression of NM23-H1 WT or NM23-H1 DN mutant. Total ARF6 and ARF6-GTP were visualized by immunoblot analysis with an anti-ARF6 mouse mAb. Densitometric analysis of ARF6-GTP is displayed as a histogram after normalizing to the expression of total ARF6 present in each sample.

24), and our present results support the idea that the ARF6 activation by cytohesin ARF GEFs is required for HCG-induced HLHCGR internalization.

Our previous studies implicated PI3K in ARF6 activation (19, 20). Consistent with this view, Wortmannin (PI3K inhibitor) reduced HCG-stimulated HLHCGR internalization. These results are similar to those obtained in HEK293 cells exogenously expressing the β2-AR where inhibition of PI3K activity with Wortmannin caused a dramatic decrease in receptor internalization (36). Gallein, a G$\beta\gamma$ inhibitor, also reduced HCG-stimulated HLHCGR internalization and was shown to inhibit G$\beta\gamma$-dependent PI3K-regulated chemokine receptor activity (38, 39). The PI3Kγ isoform is activated by G$\beta\gamma$, and therefore it is possible that this isoform of PI3K is involved in the receptor internalization (55). Wortmannin and Gallein also reduced ARF6 activation in HEK-HLHCGR cells stimulated with HCG, which correlated with the inhibition of receptor internalization by these agents and suggesting that G$\beta\gamma$-dependent PI3K-activation occurs upstream of ARF6 activation in the HLHCGR trafficking pathway.

Cytohesins 1–3 translocate from cytosol to the plasma membrane in a PI3K-dependent manner, where they activate ARF6 (20, 21, 53). Since agonist binding to HLHCGR results in ARF6 activation, we assessed whether cytohesin 2 translocates to the plasma membrane in HCG-stimulated HEK-HLHCGR cells. Cytohesin 2 translocated in those cells stimulated with HCG, and the translocation was blocked by Wortmannin and Gallein but not by SecinH3. Cytohesin 2 translocates to the plasma membrane by binding via its PH domain to PIP3, which is produced by PI3K (20). Wortmannin and Gallein will inhibit PI3K activation whereas SecinH3 only inhibits cytohesin 2 GEF activity. Therefore the former two inhibitors would be predicted to inhibit cytohesin 2 translocation whereas SecinH3 would not, as was the case. Our studies indicate that Wortmannin and Gallein inhibit HCG-induced internalization by blocking cytohesin translocation whereas SecinH3 reduced the internalization by inhibiting cytohesin ARF GEF activity. Since cytohesins translocate before activating ARF6, we can conclude that G$\beta\gamma$ and PI3K act upstream of ARF6 activation by cytohesin(s) in the ARF6 signaling pathway associated with HLHCGR internalization.

HLHCGR undergoes clathrin- and dynamin-mediated internalization in HCG-stimulated cells. EPS15 was first identified as a substrate of EGFR kinase (56), but was subsequently found to participate in clathrin-mediated endocytosis through interaction with the clathrin adaptor protein AP2, and could mediate clathrin-coated pit formation (57). The DN mutant of EPS15 decreased HLHCGR internalization and in addition led to increased agonist-stimulated cAMP production. The dynamin inhibitor, Dynasore, also decreased HCG-induced HLHCGR internalization. This finding was similar to the observation of Macia *et al.* (46), where transferrin receptor

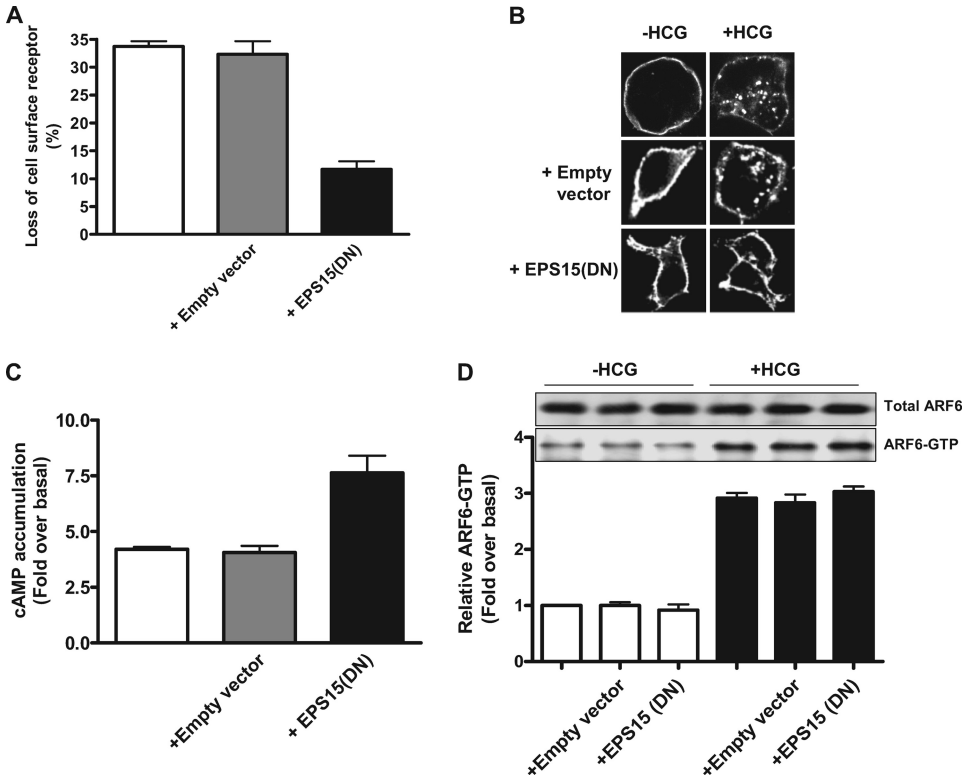

FIGURE 8. **Effect of EPS15 DN mutant on HCG-induced HLHCGR internalization and cAMP accumulation.** *A*, HEK-HLHCGR cells coexpressing empty vector or EPS15 DN plasmid were assayed by ELISA for surface receptor levels both in the absence and in the presence of HCG (10 IU/ml, 30 min). The EPS15 DN construct decreased HCG-induced HLHCGR as compared with cells that were not transfected or were transfected with empty control vector. *B*, immunofluorescence analysis showing the inhibition of HCG-stimulated (10 IU/ml HCG, 30 min) HLHCGR redistribution by coexpression of EPS15 DN mutant. *C*, cAMP production was increased in HCG-stimulated HEK-HLHCGR cells expressing EPS15 DN mutant as compared with cells expressing either not transfected or transfected with empty vector. *D*, using a GST-GGA3 PBD pulldown assay, the levels of endogenous ARF6-GTP under basal conditions and in the presence of HCG (10 IU/ml, 30 min) were not affected by coexpression of EPS15 DN mutant. Total ARF6 and ARF6-GTP were visualized by immunoblot analysis with an anti-ARF6 mouse mAb. Densitometric analysis of ARF6-GTP is displayed as a histogram after normalizing to the expression of total ARF6 present in each sample.

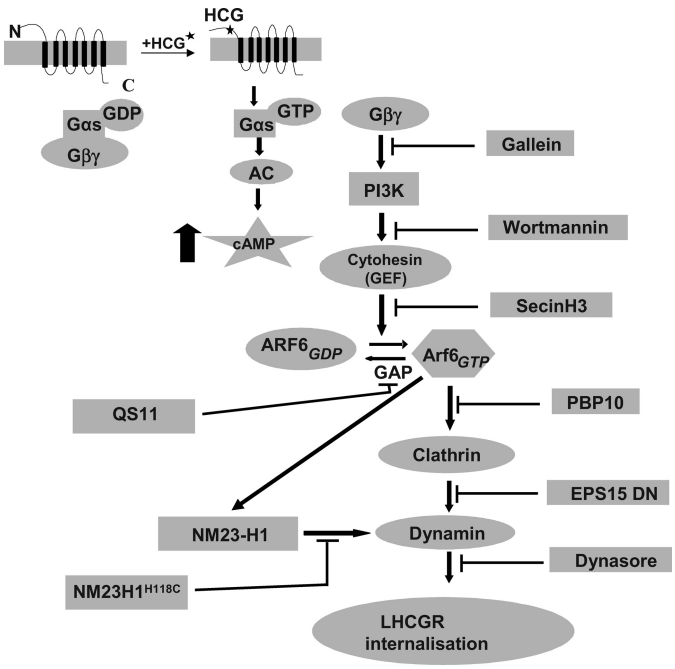

FIGURE 9. **Schematic representation of the ARF6 signaling pathway involved in HLHCGR internalization as deduced from the present study.**

trafficking was inhibited by Dynasore treatment of HeLa cells. NM23-H1 plays an important role in endocytosis by providing the GTP required for dynamin-dependent fission of coated vesicles (43, 58). The NM23-H1 DN mutant inhibited agonist-induced HLHCGR internalization and increased cAMP production, indicating that NM23-H1 is important for HCG-stimulated HLHCGR internalization. The ARF6-GTP activates PIP5K, leading to a large increase in PIP2 at the cell surface (44, 45). PIP2 then recruits AP-2 to clathrin-coated pits, suggesting a role for ARF6-GTP in clathrin-mediated endocytosis. PBP10, a membrane permeable PIP2 binding peptide, inhibits clathrin-mediated endocytosis by preventing AP2 binding to PIP2. PBP10 decreased HCG-induced LHCGR internalization with a concomitant increase in cAMP accumulation. Therefore from the results obtained using Dynasore, PBP10, NM23-H1 DN, and EPS15 DN, we can conclude that HCG-induced HLHCGR internalization occurs through the clathrin/dynamin-dependent pathway. However, none of these agents interfered with HCG-stimulated ARF6 activation, suggesting importantly that ARF6 is functioning upstream of these proteins *in vivo*.

In conclusion we find that ARF6 activation and HCG-induced HLHCGR internalization are inhibited by Gallein (G$\beta\gamma$ inhibitor), Wortmannin (PI3-K inhibitor), SecinH3 (cytohesin ARF GEF inhibitor), the ARF6 inhibitory peptide, and siRNA-mediated down-regulation of ARF6, but not by QS11

(an ARF GAP inhibitor). However Dynasore (dynamin inhibitor), PBP10 (PIP2 inhibitory peptide) and the DN mutants of NM23-H1 and EPS15 inhibited agonist-induced HLHCGR internalization but not ARF6 activation. These results suggest that the agonist binding to LHCGR results in Gαs activation, which then dissociates from G$\beta\gamma$ and activates adenylyl cyclase. G$\beta\gamma$ activates PI3K to produce the second messenger PIP3, which recruits cytohesin ARF GEFs to the membrane for ARF6 activation. We suggest that ARF6-GTP then activates PIP5K to produce PIP2, which recruits AP2 required for clathrin-coated pit assembly. ARF6-GTP also recruits NM23-H1 to clathrin-coated pits to provide GTP to dynamin dependent fission of clathrin-coated vesicles (see explanatory diagram, Fig. 9). These findings increase our understanding of the molecular mechanisms underlying the ARF6-dependent regulation of agonist-induced internalization of LHCGR, which is the most important contributor to the down-regulation of the receptor. In addition we suggest that the pathway described is likely to be utilized by a range of GPCRs and thus be of general relevance to receptor signaling and trafficking in cells.

Acknowledgments—We thank Prof. Mario Ascoli (Iowa University, IA) for kindly providing an expression plasmid encoding Myc-tagged human LHCGR. We also thank Prof. Sylvain Bourgoin (Laval University, Quebec, Canada) for providing an anti-ARF1 antibody. We are grateful to Dr Keya Saha for laboratory help. We also thank members of the VK, EK, and ALB laboratories for critically reviewing the manuscript and helping by providing various reagents necessary for the study.

REFERENCES

1. Oldham, W. M., and Hamm, H. E. (2008) Heterotrimeric G protein activation by G-protein-coupled receptors. *Nat. Rev. Mol. Cell Biol.* **9,** 60–71
2. Smrcka, A. V. (2008) G protein $\beta\gamma$ subunits: central mediators of G protein-coupled receptor signaling. *Cell Mol. Life Sci.* **65,** 2191–2214
3. Taniguchi, C. M., Emanuelli, B., and Kahn, C. R. (2006) Critical nodes in signaling pathways: insights into insulin action. *Nat. Rev. Mol. Cell Biol.* **7,** 85–96
4. Hawkins, P. T., and Stephens, L. R. (2007) PI3Kγ is a key regulator of inflammatory responses and cardiovascular homeostasis. *Science* **318,** 64–66
5. Okada, T., Kawano, Y., Sakakibara, T., Hazeki, O., and Ui, M. (1994) Essential role of phosphatidylinositol 3-kinase in insulin-induced glucose transport and antilipolysis in rat adipocytes. Studies with a selective inhibitor wortmannin. *J. Biol. Chem.* **269,** 3568–3573
6. Ascoli, M., Fanelli, F., and Segaloff, D. L. (2002) The lutropin/choriogonadotropin receptor, a 2002 perspective. *Endocr. Rev.* **23,** 141–174
7. Wang, H., Segaloff, D. L., and Ascoli, M. (1991) Lutropin/choriogonadotropin down-regulates its receptor by both receptor-mediated endocytosis and a cAMP-dependent reduction in receptor mRNA. *J. Biol. Chem.* **266,** 780–785
8. Hanyaloglu, A. C., and von Zastrow, M. (2008) Regulation of GPCRs by endocytic membrane trafficking and its potential implications. *Annu. Rev. Pharmacol. Toxicol.* **48,** 537–568
9. Gurevich, V. V., and Gurevich, E. V. (2006) The structural basis of arrestin-mediated regulation of G-protein-coupled receptors. *Pharmacol. Ther.* **110,** 465–502
10. Min, L., and Ascoli, M. (2000) Effect of activating and inactivating mutations on the phosphorylation and trafficking of the human lutropin/choriogonadotropin receptor. *Mol. Endocrinol.* **14,** 1797–1810
11. Hunzicker-Dunn, M., Gurevich, V. V., Casanova, J. E., and Mukherjee, S. (2002) ARF6: a newly appreciated player in G protein-coupled receptor desensitization. *FEBS Lett.* **521,** 3–8
12. Moss, J., and Vaughan, M. (1998) Molecules in the ARF orbit. *J. Biol. Chem.* **273,** 21431–21434
13. Donaldson, J. G., Finazzi, D., and Klausner, R. D. (1992) Brefeldin A inhibits Golgi membrane-catalyzed exchange of guanine nucleotide onto ARF protein. *Nature* **360,** 350–352
14. Zeeh, J. C., Zeghouf, M., Grauffel, C., Guibert, B., Martin, E., Dejaegere, A., and Cherfils, J. (2006) Dual specificity of the interfacial inhibitor brefeldin a for arf proteins and sec7 domains. *J. Biol. Chem.* **281,** 11805–11814
15. Hafner, M., Schmitz, A., Grüne, I., Srivatsan, S. G., Paul, B., Kolanus, W., Quast, T., Kremmer, E., Bauer, I., and Famulok, M. (2006) Inhibition of cytohesins by SecinH3 leads to hepatic insulin resistance. *Nature* **444,** 941–944
16. Zhang, Q., Major, M. B., Takanashi, S., Camp, N. D., Nishiya, N., Peters, E. C., Ginsberg, M. H., Jian, X., Randazzo, P. A., Schultz, P. G., Moon, R. T., and Ding, S. (2007) Small-molecule synergist of the Wnt/β-catenin signaling pathway. *Proc. Natl. Acad. Sci. U.S.A.* **104,** 7444–7448
17. Venkateswarlu, K., Oatey, P. B., Tavaré, J. M., Jackson, T. R., and Cullen, P. J. (1999) Identification of centaurin-α1 as a potential in vivo phosphatidylinositol 3,4,5-trisphosphate-binding protein that is functionally homologous to the yeast ADP-ribosylation factor (ARF) GTPase-activating protein, Gcs1. *Biochem. J.* **340**, 359–363
18. Venkateswarlu, K., Gunn-Moore, F., Oatey, P. B., Tavaré, J. M., and Cullen, P. J. (1998) Nerve growth factor- and epidermal growth factor-stimulated translocation of the ADP-ribosylation factor-exchange factor GRP1 to the plasma membrane of PC12 cells requires activation of phosphatidylinositol 3-kinase and the GRP1 pleckstrin homology domain. *Biochem. J.* **335**, 139–146
19. Venkateswarlu, K., Oatey, P. B., Tavaré, J. M., and Cullen, P. J. (1998) Insulin-dependent translocation of ARNO to the plasma membrane of adipocytes requires phosphatidylinositol 3-kinase. *Curr. Biol.* **8,** 463–466
20. Cullen, P. J., and Venkateswarlu, K. (1999) Potential regulation of ADP-ribosylation factor 6 signaling by phosphatidylinositol 3,4,5-trisphosphate. *Biochem. Soc Trans.* **27,** 683–689
21. Venkateswarlu, K., and Cullen, P. J. (2000) Signalling via ADP-ribosylation Factor G lies downstream of phosphatidylinositide 3-kinase. *Biochem. J.* **345,** 719–724
22. Claing, A. (2004) Regulation of G protein-coupled receptor endocytosis by ARF6 GTP-binding proteins. *Biochem. Cell Biol.* **82,** 610–617
23. Venkateswarlu, K., Brandom, K. G., and Lawrence, J. L. (2004) Centaurin-alpha1 is an in vivo phosphatidylinositol 3,4,5-trisphosphate-dependent GTPase-activating protein for ARF6 that is involved in actin cytoskeleton organization. *J. Biol. Chem.* **279,** 6205–6208
24. Lawrence, J., Mundell, S. J., Yun, H., Kelly, E., and Venkateswarlu, K. (2005) Centaurin-α1, an ADP-ribosylation factor 6 GTPase-activating protein, inhibits β2-adrenoceptor internalization. *Mol. Pharmacol.* **67,** 1822–1828
25. Venkateswarlu, K. (2003) Interaction protein for cytohesin exchange factors 1 (IPCEF1) binds cytohesin 2 and modifies its activity. *J. Biol. Chem.* **278,** 43460–43469
26. Benmerah, A., Bayrou, M., Cerf-Bensussan, N., and Dautry-Varsat, A. (1999) Inhibition of clathrin-coated pit assembly by an Eps15 mutant. *J. Cell Sci.* **112**, 1303–1311
27. Volpicelli-Daley, L. A., Li, Y., Zhang, C. J., and Kahn, R. A. (2005) Isoform-selective effects of the depletion of ADP-ribosylation factors 1–5 on membrane traffic. *Mol. Biol. Cell* **16,** 4495–4508
28. Hashimoto, S., Onodera, Y., Hashimoto, A., Tanaka, M., Hamaguchi, M., Yamada, A., and Sabe, H. (2004) Requirement for Arf6 in breast cancer invasive activities. *Proc. Natl. Acad. Sci. U.S.A.* **101,** 6647–6652
29. Venkateswarlu, K. (2005) Analysis of the interaction between cytohesin 2 and IPCEF1. *Methods Enzymol.* **404,** 252–266
30. Galas, M. C., Helms, J. B., Vitale, N., Thiersé, D., Aunis, D., and Bader, M. F. (1997) Regulated exocytosis in chromaffin cells. A potential role for a secretory granule-associated ARF6 protein. *J. Biol. Chem.* **272,** 2788–2793
31. Derossi, D., Chassaing, G., and Prochiantz, A. (1998) Trojan peptides: the penetratin system for intracellular delivery. *Trends Cell Biol.* **8,** 84–87
32. Kagan, J. C., and Medzhitov, R. (2006) Phosphoinositide-mediated adap-

tor recruitment controls Toll-like receptor signaling. *Cell* **125,** 943–955
33. Klausner, R. D., Donaldson, J. G., and Lippincott-Schwartz, J. (1992) Brefeldin A: insights into the control of membrane traffic and organelle structure. *J. Cell Biol.* **116,** 1071–1080
34. Abel, K., Anderson, R. A., and Shears, S. B. (2001) Phosphatidylinositol and inositol phosphate metabolism. *J. Cell Sci.* **114,** 2207–2208
35. Stephens, L., Smrcka, A., Cooke, F. T., Jackson, T. R., Sternweis, P. C., and Hawkins, P. T. (1994) A novel phosphoinositide 3 kinase activity in myeloid-derived cells is activated by G protein $\beta\gamma$ subunits. *Cell* **77,** 83–93
36. Naga Prasad, S. V., Barak, L. S., Rapacciuolo, A., Caron, M. G., and Rockman, H. A. (2001) Agonist-dependent recruitment of phosphoinositide 3-kinase to the membrane by β-adrenergic receptor kinase 1. A role in receptor sequestration. *J. Biol. Chem.* **276,** 18953–18959
37. Yano, H., Nakanishi, S., Kimura, K., Hanai, N., Saitoh, Y., Fukui, Y., Nonomura, Y., and Matsuda, Y. (1993) Inhibition of histamine secretion by wortmannin through the blockade of phosphatidylinositol 3-kinase in RBL-2H3 cells. *J. Biol. Chem.* **268,** 25846–25856
38. Lehmann, D. M., Seneviratne, A. M., and Smrcka, A. V. (2008) Small molecule disruption of G protein $\beta\gamma$ subunit signaling inhibits neutrophil chemotaxis and inflammation. *Mol. Pharmacol.* **73,** 410–418
39. Bonacci, T. M., Mathews, J. L., Yuan, C., Lehmann, D. M., Malik, S., Wu, D., Font, J. L., Bidlack, J. M., and Smrcka, A. V. (2006) Differential targeting of G$\beta\gamma$-subunit signaling with small molecules. *Science* **312,** 443–446
40. Venkateswarlu, K., Gunn-Moore, F., Tavaré, J. M., and Cullen, P. J. (1999) EGF-and NGF-stimulated translocation of cytohesin-1 to the plasma membrane of PC12 cells requires PI 3-kinase activation and a functional cytohesin-1 PH domain. *J. Cell Sci.* **112**, 1957–1965
41. Lazari, M. F., Bertrand, J. E., Nakamura, K., Liu, X., Krupnick, J. G., Benovic, J. L., and Ascoli, M. (1998) Mutation of individual serine residues in the C-terminal tail of the lutropin/choriogonadotropin receptor reveal distinct structural requirements for agonist-induced uncoupling and agonist-induced internalization. *J. Biol. Chem.* **273,** 18316–18324
42. D'Souza-Schorey, C., and Chavrier, P. (2006) ARF proteins: roles in membrane traffic and beyond. *Nat. Rev. Mol. Cell Biol.* **7,** 347–358
43. Palacios, F., Schweitzer, J. K., Boshans, R. L., and D'Souza-Schorey, C. (2002) ARF6-GTP recruits Nm23-H1 to facilitate dynamin-mediated endocytosis during adherens junctions disassembly. *Nat. Cell Biol.* **4,** 929–936
44. Krauss, M., Kinuta, M., Wenk, M. R., De Camilli, P., Takei, K., and Haucke, V. (2003) ARF6 stimulates clathrin/AP-2 recruitment to synaptic membranes by activating phosphatidylinositol phosphate kinase type Iγ. *J. Cell Biol.* **162,** 113–124
45. Paleotti, O., Macia, E., Luton, F., Klein, S., Partisani, M., Chardin, P., Kirchhausen, T., and Franco, M. (2005) The small G-protein Arf6GTP recruits the AP-2 adaptor complex to membranes. *J. Biol. Chem.* **280,** 21661–21666
46. Macia, E., Ehrlich, M., Massol, R., Boucrot, E., Brunner, C., and Kirchhausen, T. (2006) Dynasore, a cell-permeable inhibitor of dynamin. *Dev. Cell* **10,** 839–850
47. Fu, H., Björkman, L., Janmey, P., Karlsson, A., Karlsson, J., Movitz, C., and Dahlgren, C. (2004) The two neutrophil members of the formylpeptide receptor family activate the NADPH-oxidase through signals that differ in sensitivity to a gelsolin-derived phosphoinositide-binding peptide. *BMC Cell Biol.* **5,** 50
48. Bhaskaran, R. S., and Ascoli, M. (2005) The post-endocytotic fate of the gonadotropin receptors is an important determinant of the desensitization of gonadotropin responses. *J. Mol. Endocrinol.* **34,** 447–457
49. Poupart, M. E., Fessart, D., Cotton, M., Laporte, S. A., and Claing, A. (2007) ARF6 regulates angiotensin II type 1 receptor endocytosis by controlling the recruitment of AP-2 and clathrin. *Cell Signal.* **19,** 2370–2378
50. Claing, A., Chen, W., Miller, W. E., Vitale, N., Moss, J., Premont, R. T., and Lefkowitz, R. J. (2001) β-Arrestin-mediated ADP-ribosylation factor 6 activation and β2-adrenergic receptor endocytosis. *J. Biol. Chem.* **276,** 42509–42513
51. Houndolo, T., Boulay, P. L., and Claing, A. (2005) G protein-coupled receptor endocytosis in ADP-ribosylation factor 6-depleted cells. *J. Biol. Chem.* **280,** 5598–5604
52. Svensson, H. G., West, M. A., Mollahan, P., Prescott, A. R., Zaru, R., and Watts, C. (2008) A role for ARF6 in dendritic cell podosome formation and migration. *Eur. J. Immunol.* **38,** 818–828
53. Frank, S., Upender, S., Hansen, S. H., and Casanova, J. E. (1998) ARNO is a guanine nucleotide exchange factor for ADP-ribosylation factor 6. *J. Biol. Chem.* **273,** 23–27
54. Mukherjee, S., Gurevich, V. V., Jones, J. C., Casanova, J. E., Frank, S. R., Maizels, E. T., Bader, M. F., Kahn, R. A., Palczewski, K., Aktories, K., and Hunzicker-Dunn, M. (2000) The ADP ribosylation factor nucleotide exchange factor ARNO promotes β-arrestin release necessary for luteinizing hormone/choriogonadotropin receptor desensitization. *Proc. Natl. Acad. Sci. U.S.A.* **97,** 5901–5906
55. Rameh, L. E., and Cantley, L. C. (1999) The role of phosphoinositide 3-kinase lipid products in cell function. *J. Biol. Chem.* **274,** 8347–8350
56. Fazioli, F., Minichiello, L., Matoskova, B., Wong, W. T., and Di Fiore, P. P. (1993) eps15, a novel tyrosine kinase substrate, exhibits transforming activity. *Mol. Cell. Biol.* **13,** 5814–5828
57. Chen, H., Slepnev, V. I., Di Fiore, P. P., and De Camilli, P. (1999) The interaction of epsin and Eps15 with the clathrin adaptor AP-2 is inhibited by mitotic phosphorylation and enhanced by stimulation-dependent dephosphorylation in nerve terminals. *J. Biol. Chem.* **274,** 3257–3260
58. Di Fiore, P. P., and De Camilli, P. (2001) Endocytosis and signaling. an inseparable partnership. *Cell* **106,** 1–4

Supplemental Figures

Figure S1. Concentration- and time-dependent internalisation of HLHCGR and cAMP production in HEK-HLHCGR cells stimulated with HCG. A. HCG-stimulated loss of cell surface HLHCGR as determined by ELISA. Cells were incubated with (i) different concentrations of HCG for 30 min or 10 IU/ml HCG for 0-60 min. Open symbols indicate cells incubated in the absence of HCG. **B.** Immunofluorescence analysis of HLHCGR internalisation in cells incubated with or without agonist as shown. HEK-HLHCGR cells were incubated with an anti-Myc mouse mAb at 4°C and then incubated without (-HCG) or with 10 IU/ml HCG (+HCG) for 60 min (i) or with HCG at the indicated concentrations for 30min or 10 IU/ml HCG for 0-60 min (iii) at 37°C. The cells were then fixed, permeabilised and immunostained using FITC-conjugated anti-mouse secondary antibody and the staining visualised by confocal microscopy. **C.** Concentration- and time dependent cAMP accumulation by HCG. Cells were incubated with (i) different concentrations of HCG for 30 min or 10 IU/ml HCG for 0-60 min. Open symbols indicate cells incubated in the absence of HCG.The concentration- and time- dependence of HCG-stimulated cAMP production. HEK-HLHCGR were serum starved and stimulated without (○) or with HCG (●) at a concentration of 0.01-1000 IU/ml for 30 min (i) or 10 IU/ml for 0-60 min.

Figure S2. Effect of QS11 (ARF GAP inhibitor) and BFA on HCG-induced HLHCGR internalisation and cAMP accumulation. A. HEK-HLHCGR cells pre-incubated with either BFA (1-50μg/ml, □, ■) or QS11 (0.1-12.5μM, Δ, ▲) for 30 min at 37°C were incubated without (open symbols) or with (solid symbols) 10 IU/ml HCG for 30 min at 37°C and receptor internalisation determined by ELISA. **B.** Immunofluorescence analysis of the effect of QS11 and BFA on HCG-stimulated (10 IU/ml HCG, 30 min) HLHCGR internalisation. **C.** cAMP accumulation in unstimulated (open symbols) or HCG-stimulated (solid symbols; 10 IU/ml HCG, 30 min) HEK-HLHCGR cells pretreated with the indicated concentrations of BFA or QS11 as described in part A above.

Figure S3. Effect of QS11 on ARF6 activation in HCG-stimulated HEK-HLHCGR cells. HCG-stimulated (10 IU/ml HCG, 30 min) ARF6 activation was assessed by a GST-GGA3 PBD pull down assay in HEK-HLHCGR cells preincubated with the indicated concentrations of QS11. Total ARF6 levels in the cell lysate and the resin bound ARF6-GTP were visualised by immunoblot analysis with an anti-ARF6 mouse mAb. Densitometric analysis of ARF6-GTP is shown as a histogram after normalising to the expression of total ARF6 present in the sample. Solid bars indicate measurements made in the presence of HCG.

Figure S4. Effect of Dynasore on HCG-induced HLHCGR internalisation and cAMP accumulation. A. HEK-HLHCGR cells were preincubated with Dynasore (16-400 μM) for 15 min at 37°C, and were assayed by ELISA for loss of the cell surface receptor both in the absence (□) and in the presence (■) of 10 IU/ml HCG, 30 min. **B.** Immunofluorescence analysis showing the inhibition of HCG-stimulated (10 IU/ml HCG, 30 min) HLHCGR redistribution by 80 μM Dynasore. **C.** Concentration-dependent effect of Dynasore on cAMP accumulation in HEK-HLHCGR cells incubated without (Δ) or with (▲) 10 IU/ml HCG for 30 min. **D.** Using a GST-GGA3 PBD pull down assay, the levels of endogenous ARF6-GTP under basal conditions and in the presence of HCG (10 IU/ml HCG, 30 min) were not affected by Dynasore. Total ARF6 and ARF6-GTP were visualised by immunoblot analysis with an anti-ARF6 mouse mAb. Densitometric analysis of ARF6-GTP is displayed as a histogram after normalising to the expression of total ARF6 present in each sample.

Figure S5. Effect of PBP10 on HCG-induced HLHCGR internalisation and cAMP accumulation. A. HEK-HLHCGR cells preincubated with PBP10 (0.01-10μM) for 15 min at 37°C were assayed by ELISA for loss of surface receptor both in the absence (□) and presence (■) of HCG (10 IU/ml HCG, 30 min).. **B.** Immunofluorescence analysis showing the inhibition of HCG-

stimulated (10 IU/ml HCG, 30 min) HLHCGR redistribution by 1 μM PBP10. **C.** Effect of PBP10 (0.001-10 μM) on cAMP accumulation in unstimulated (Δ) or 10 IU/ml HCG-stimulated (▲) HEK-HLHCGR cells. PBP10 had a concentration-dependent stimulatory effect on HCG-induced cAMP accumulation. **D.** Using a GST-GGA3 PBD pull down assay, the levels of endogenous ARF6-GTP under basal conditions and in the presence of HCG (10 IU/ml HCG, 30 min) were not affected by PBP10. Total ARF6 and ARF6-GTP were visualised by immunoblot analysis with an anti-ARF6 mouse mAb. Densitometric analysis of ARF6-GTP is displayed as a histogram after normalising to the expression of total ARF6 present in each sample.